CHAPTER 7
RADIOLABELING AND BIODISTRIBUTION STUDIES

7. RADIOLABELING AND BIODISTRIBUTION STUDIES

7.1 Introduction

Labeling of the liposomes with radioisotopes is carried out by entrapping the suitable gamma emitting radioisotope such as ^{99m}Tc. Two approaches for radiolabeling have been reported one is by attachment of the label to the lipid component prior to liposome preparation and another way is to radiolabel the liposome after manufacturing (Richardson et al., 1978). Radiolabeled liposome have been successfully used for preclinical evaluation of pharmacokinetic parameters of liposomal delivery system as this can be administered to animals by different routes and its uptake in various organs can be estimated with time. Radiolabeled liposome preparations have also been used successfully for imaging tumor, abscesses, ischemia and infracted region.

Liposomes can be labeled using various isotopes among them Technetium 99m (^{99m}Tc) is used widely due to its easy availability from Molybdenum-99 (^{99}Mo) - ^{99m}Tc generator and its favorable physical characteristics such as convenient short half life of (6 hrs), 140KeV gamma energy which is ideal for detection with current instruments. No particulate emission that decrease the radiation burden to the patient. Hence 99mTc has become the choice of isotope for nuclear medicine and currently ^{99m}Tc radiopharmaceuticals are available for imaging all major organs such as bone, liver, kidney, brain, heart etc. Various drug delivery systems such as liposomes, gastro-retentive floating drug delivery systems, solid lipid dosage forms and colonic drug delivery systems have been currently evaluated using ^{99m}Tc.

7.2 Technetium Chemistry

Technetium (atomic number 43) a transition metal element belongs to group VIIB of the periodic table. ^{99m}Tc can exist in eight oxidation namely 1^- to 7^+ among the 7^+ and 4^+ are the most stable state and are represented in oxides, sulphides, halides and pertechnetate. The chemical form of ^{99m}Tc from Molybdenum generator is available as sodium pertechnetate (^{99m}Tc-$NaTCO_4$). The pertechnetate ion, $^{99m}TcO_4$- has the oxidation state 7^+, that resembles the permanganate ions Mn O_4-. Pertechnetate is non-reactive and it is not possible to label any compound by direct addition of pertechnetate, so prior to labeling reduction of ^{99m}Tc from 7^+ state to lower oxidation

is required (Saha 1993). Among the various reducing agents stannous ions in the form of chloride, tartarate is commonly used in acidic medium. The reduced ^{99m}Tc species are chemically reactive and combine with wide variety of ligands bearing chemical groups such as –COOH, -OH, $-NH_2$, and –SH as N,S, O act as good donor atoms for ^{99m}Tc. Other methods of labeling via HMPAO, or HYNIC are also reported in literature for liposomes.

7.3 Biodistribution and tumor targeting of liposomes

The pharmacokinetics and tissue distribution of liposomes after parenteral administration are determined by a diversity of variables, including liposome size and composition, stearic stabilization of the liposome, presence of surface-grafted molecules, such as targeting devices and obviously, the organism and the health status of that particular organism. Closely related to this last point is the accessibility of target tissues or cells for the liposomes. Upon injection, liposomes encounter anatomical barriers such as the endothelial lining of the vasculature and also of the blood-brain barrier, which will prevent access of the liposomes to extravascular sites. Only in organs such as the liver (see also later), spleen, bone marrow and under certain pathological conditions, such as occurring in solid tumors and at sites of infection or inflammation, the vascular endothelium may display enhanced permeability, allowing liposomes to extravasate (Ishida et al., 1999; Maruyama, 2000). The surface properties of particulate carriers greatly define their *in vivo* fate. The extent of blood clearance depend on the physicochemical properties of the particles, such as size, surface charge and surface hydrophobicity. The charge and the surface property carried by the colloidal particles can have an important role in determining the clearance and fate of the particles (Laverman et al., 1999).

Radiolabels, either encapsulated water-soluble compounds or bilayer-incorporated lipid labels, provide a sensitive and powerful tool to determine liposome biodistribution. These markers provide a convenient way for a rapid and quantitative assessment of tissue distribution after parenteral administration of liposomes and produce reliable and reproducible data on tissue distribution both shortly after injection (1–4 h) and at longer times after injection (24 hrs). Apart from quantifying the radioactivity and estimating the percentage distribution in various organs it can

also used to visualize the biodistribution of liposome without sacrificing the animal by gamma scintigraphic imaging. Biodistribution of liposome used can provide the information on localization of the carrier system in various organs which are have be intended to target the specific site (Kamps and Scherphof, 2004).

Here we have studied the biodistribution of the developed liposomal delivery system in various organs after intravenous injection into mice and mice bearing solid tumor. We have compared the conventional, stealth and folate targeted liposomes, for targeting ability to folate receptor and biodistribution in female swiss mice and tumor induced mice.

7.4 Experimental

7.4.1 Materials

Stannous chloride dihydrate ($SnCl_2.2H_2O$) was purchased from Sigma Chemical Co.(St. Louis, MO), sodium pertechnetate, separated from molybdenom-99 (99m) by solvent extraction method, was provided by Regional Center for Radiopharmaceutical Division (Northern Region) Board of Radiation and Isotope Technology (BRIT, Delhi, India).

7.4.2 Preparation and characterization of formulations

The liposomal formulations (pure drug PD, Conventional CL, Stealth SL and Folate targeted FT) of gemcitabine (GEM) were prepared as described in section 4.2.3 and characterized as described in section 4.2.3. The formulations listed in the Table 4.2.3 were taken for the biodistribution study.

7.5 Radiolabeling of formulations and optimization

The formulations were radiolabeled using technetium-99m (^{99m}Tc) by direct-labeling method (Eckelman et al., 1995; Babbar et al., 2000). Radiolabeled technetium in sodium pertechnetate was reduced in the acidic medium in the presence of stannous chloride.

For carrying out the radiolabelling of the formulations, the required volume of formulation was treated with stannous chloride in 0.1N hydrochloric acid and the pH was adjusted with sodium bicarbonate solution. Sterile sodium per ^{99m}Tc-

pertechnetate (35 to 40 mCi/mL) was added with continuous mixing such that the resultant solution has the required radioactivity for the animal studies. The mixture was incubated at 30°C ± 5°C for 10 minutes. The final required volume was made up with 0.9 %w/v sterile sodium chloride solution.

Generally technetium is reduced in the presence of formulations, which enable the formulations tagged with technetium. In certain case, the previously reduced technetium is used for tagging of the formulations. The radiochemical purity of the formulations was determined using ascending instant thin layer chromatography (TLC). Silica gel-coated fiberglass sheets (Gelman Sciences Inc, Ann Arbor, MI) were used as stationary phase while dual solvent systems consisting of acetone and pyridine: acetic acid: water (3:5:1.5 v/v) were used as mobile phases (Saha, 1993; Saha, 2005). Since the free technetium is having R_f value of nearly 1 in acetone mobile phase, the ratio of radioactivity in the top $1/3^{rd}$ to lower $2/3^{rd}$ of the ITLC plates were used as the index of the percentage labeled. The contaminants redued/ hydrolysed (^{99m}Tc) collectively were called as colloids which were identified by their lower R_f values in pyridine: acetic acid: water (3:5:1.5 v/v) mobile phase.

The effect of incubation time, pH, and stannous chloride concentration on labeling were studied to achieve optimum labeling of the formulations and were tabulated. The *in-vitro* stability of radiolabeled formulations was evaluated in 0.9%w/v sodium chloride (normal saline) and mice serum by ascending ITLC (Garron et al., 1991).

To evaluate stability and bonding strength of the labeled complex, the radio labeld formulations were challenged against various concentrations (1,2,3 and 4mM) of Diethylene Triamine Penta acetic acid (DTPA). Since ^{99m}Tc- DTPA complex have higher R_f values in pyridine: acetic acid: water (3:5:1.5 v/v) mobile phase, where the radiolabeled formulations retained at point of application. The effect of different molar concentrations and percent transchelation on radiolabeled formulations was tabulated. The optimized radiolabelled formulations were assessed for *in vitro* stability in normal saline and in mice serum (Theobald, 1990). Consequently, the optimized stable radiolabeled formulations were used for *in vivo* studies.

7.6 Biodistribution Studies

The Social Justice and Empowerment Committee, Ministry of Government of India, approved all animal experiments were conducted for the purpose of control and supervision on animals and experiments. Swiss mice (aged 6 to 8 weeks), weighing between 20 to 25g, Swiss mice bearing desire size tumor (~1to 1.5cm), and without tumor were selected for the study. Three mice for each formulation per time point were used in this study. Radiolabeled complex of ^{99m}Tc-formulations of 100 µL of radiolabeled complex of ^{99m}Tc-solution was injected through tail vein of the mice. Blood was withdrawn by cardiac puncture after different time interval and the mice were sacrificed by cervical dislocation. The blood was weighed and the radioactivity present in the whole blood was calculated by keeping 7.3% of the body weight as the total blood weight (Wu et al., 1981). Major organs (heart, liver, spleen, kidney, lungs, tumor, intestine, stomach and brain) were isolated weighed and radioactivity present in each tissue/organ was measured using shielded well-type gamma scintillation counter. Radiopharmaceutical uptake per gram in each tissue/organ was calculated as a fraction of administered dose using equation:

$$\% \text{ Radioactivity /gm of tissue} = \frac{\text{counts in sample x 100}}{\text{wt of sample x total counts injected}}$$

The pharmacokinetic parameters, like AUC, liver /blood ratio in all time points were calculated. The area under the % radio activity per gram of tissue vs. time curve from zero to 24 hour (AUC) was calculated by standard trapezoidal rule. Terminal elimination rate constant (β) for drug following intravenous administration was obtained by linear regression analysis of the terminal log-linear portion of % radio activity per gram of tissue vs. time curve. The 0^{th} time concentration followed by i.v. route was calculated by interpolation of terminal elimination curve to the Y axis (Zhao, 2007).

7.7 Gamma Scintigraphy Imaging

For Scintigraphic studies, female swiss mice (weighing 20-25 g) were administered with 100 µL (1.0 mCi) of the ^{99m}Tc- liposome complex (CL, SL and FT) intravenously through the tail vein. The animal was anesthetized by using chloroform. The animals were placed on board and images were captured using single positron emission computerized tomography (SPECT, LC 75-005, Diacam, Siemens AG, Erlanger, Germany) gamma camera (Capala et al., 1997; Babbar et al., 2000). The scintigraphy images following intravenous administration of formulations were shown in Fig. 7.6.

7.8 Statistical Analysis

All data are reported as mean ± SD and the difference between the groups were tested using Student's t test at the level of $P<0.05$.

7.9 Results

7.9.1 Gemcitabine HCl Formulations

Table 7.1 Effect of quantity of $SnCl_2$ on radiolabeling of gemcitabine HCl formulations

S.No.	Amount of Stannous Chloride (µgm)	% Radiolabeled			
		PD	CL	SL	FT
1	200	85.24 ± 2.12	89.84 ± 1.89	88.65 ± 2.14	87.26 ± 2.26
2	250	90.63 ± 2.84	84.76 ± 1.85	96.43 ± 1.48	95.86 ± 2.12
3	300	92.48 ± 2.21	80.36 ± 2.15	92.46 ± 2.16	90.48 ± 2.32

Table 7.2 *In vitro* stability of labeled gemcitabine formulations

SL. No	Time	In saline				In serum			
		PD	CL	SL	FT	PD	CL	SL	FT
1	1 hr	91.46 ± 2.64	90.46 ± 2.44	92.64 ± 1.86	90.47 ± 2.24	93.21 ± 2.36	93.45 ± 2.26	95.46 ± 3.13	95.82 ± 2.68
2	4 hr	91.24 ± 1.84	92.35 ± 3.04	93.46 ± 2.24	92.61 ± 1.86	91.26 ± 1.46	91.46 ± 2.18	93.28 ± 1.08	94.26 ± 2.34
3	24 hr	90.26 ± 1.64	90.62 ± 2.16	91.46 ± 1.86	90.64 ± 2.26	89.64 ± 2.39	90.48 ± 1.96	91.14 ± 1.16	92.08 ± 2.14

Table 7.3 Effect of DTPA on radiolabeling of gemcitabine formulations

SL.No.	DTPA concentration (mM)	% Transchelation			
		PD	CL	SL	FT
1	1	1.43 ± 0.86	1.36 ± 0.38	1.26 ± 0.74	1.32 ± 0.81
2	2	2.28 ± 0.76	1.42 ± 0.46	2.04 ± 0.64	2.14 ± 0.48
3	3	3.12 ± 0.42	2.18 ± 0.74	2.36 ± 0.43	2.42 ± 0.72
4	4	3.22 ± 0.56	2.64 ± 0.38	2.49 ± 0.39	2.55 ± 0.52

Table 7.4 Radiolabelling summary of gemcitabine formulations

S.No.		PD	CL	SL	FT
1	Method	Direct labeling method	Direct labeling method	Direct labeling method	Direct labeling method
2	Amount of $SnCl_2$(4mg/mL)	300µgm	200µgm	250µgm	250µgm
3	pH	pH 6-7	pH 6.0 -7.5	pH 6.0 -7.5	pH 6.0 -7.5
4	Incubation duration	½ hr	20 min	15 min	15 min
5	Labelling efficiency (%)	91.46 ± 2.64	92.35 ± 3.04	93.46 ± 2.24	92.61 ± 1.86

Table 7.5 Biodistribution of ^{99m}Tc labeled PD, CL, SL and FT Liposomes in mice

	% I.D. per gm											
	1 hr				4 hrs				24 hrs			
Organ/Time	CL	SL	FT	PD	CL	SL	FT	PD	CL	SL	FT	PD
Blood	1.143±0.09	4.101±0.11	4.762±0.10	0.568±0.04	0.835±0.065	2.673±0.07	2.896±0.05	0.427±0.02	0.443±0.05	0.971±0.03	1.246±0.01	0.328±0.02
Heart	0.502±0.02	0.847±0.01	0.766±0.04	1.122±0.03	0.444±0.02	0.401±0.03	0.368±0.01	0.963±0.04	0.353±0.03	0.418±0.01	0.368±0.03	0.755±0.03
Lungs	1.624±0.12	2.012±0.09	1.982±0.05	1.165±0.07	0.722±0.03	0.537±0.05	0.646±0.03	0.524±0.04	0.566±0.03	0.524±0.02	0.643±0.05	0.378±0.02
Spleen	7.636±0.01	5.105±0.03	5.025±0.02	10.095±0.03	5.575±0.02	1.887±0.03	1.467±0.02	7.218±0.03	4.430±0.03	0.992±0.02	0.867±0.03	5.419±0.07
Liver	11.363±0.23	10.139±0.13	9.604±0.14	21.932±0.22	8.699±0.13	6.668±0.17	6.036±0.09	20.176±0.16	4.443±0.03	3.872±0.09	3.260±0.06	14.901±0.12
Kidney	2.330±0.09	4.270±0.04	4.893±0.07	5.142±0.07	2.406±0.02	1.864±0.03	1.864±0.04	3.835±0.03	2.505±0.05	1.399±0.03	0.986±0.03	4.423±0.04
Brain	0.051±0.01	0.092±0.01	0.067±0.02	1.067±0.01	0.049±0.01	0.118±0.01	0.218±0.01	1.063±0.02	0.092±0.01	0.133±0.03	0.187±0.02	0.141±0.01
Stomach	0.301±0.02	0.398±0.01	0.449±0.04	0.225±0.02	0.324±0.04	0.284±0.03	0.284±0.04	0.263±0.03	0.531±0.03	0.635±0.01	0.722±0.04	0.746±0.01
Intestine	0.623±0.03	0.448±0.01	0.306±0.01	1.155±0.03	0.335±0.01	0.232±0.02	0.201±0.03	0.984±0.04	0.216±0.03	0.165±0.02	0.118±0.02	0.605±0.03

***In vivo* mice were administered with ^{99m}Tc labeled PD, CL, SL and FT liposomes and the radioactivity was measured after 1, 4 and 24 hrs post injection. The values represented here are the mean of three values with ± standard deviation. Radioactivity is expressed as percent of administered dose per gram of tissue or organ**

Table 7.6 Biodistribution of ^{99m}Tc labeled CL and FT Liposomes in tumor bearing mice

	% I.D. per gm			
	1hr		24 hrs	
Organ/Time	**CL**	**FT**	**CL**	**FT**
Blood	1.249±0.20	1.489±0.41	0.410±0.07	0.520±0.09
Heart	0.309±0.04	0.209±0.03	0.130±0.03	0.130±0.04
Lungs	1.319±0.40	0.259±0.06	0.260±0.04	0.130±0.05
Spleen	3.500±0.12	3.932±0.21	0.080±0.01	0.060±0.01
Liver	40.17±1.60	25.460±1.20	3.300±0.64	2.103±0.24
Kidney	3.551±0.60	1.889±0.30	0.170±0.043	0.140±0.03
Brain	0.059±0.02	0.089±0.01	0.250±0.04	0.230±0.06
Stomach	0.384±0.06	0.309±0.06	0.160±0.05	0.120±0.04
Intestine	0.389±0.04	0.419±0.04	0.220±0.04	0.110±0.02
Tumor	0.249±0.08	2.490±0.60	0.180±0.03	0.280±0.08
Muscle	0.139±0.03	0.219±0.02	0.150±0.02	0.140±0.05

***In vivo* mice were administered with ^{99m}Tc labeled CL and FT liposomes and the radioactivity was measured after 1 and 24 hrs post injection. The values represented here are the mean of three values with ± standard deviation. Radioactivity is expressed as percent of administered dose per gram of tissue or organ**

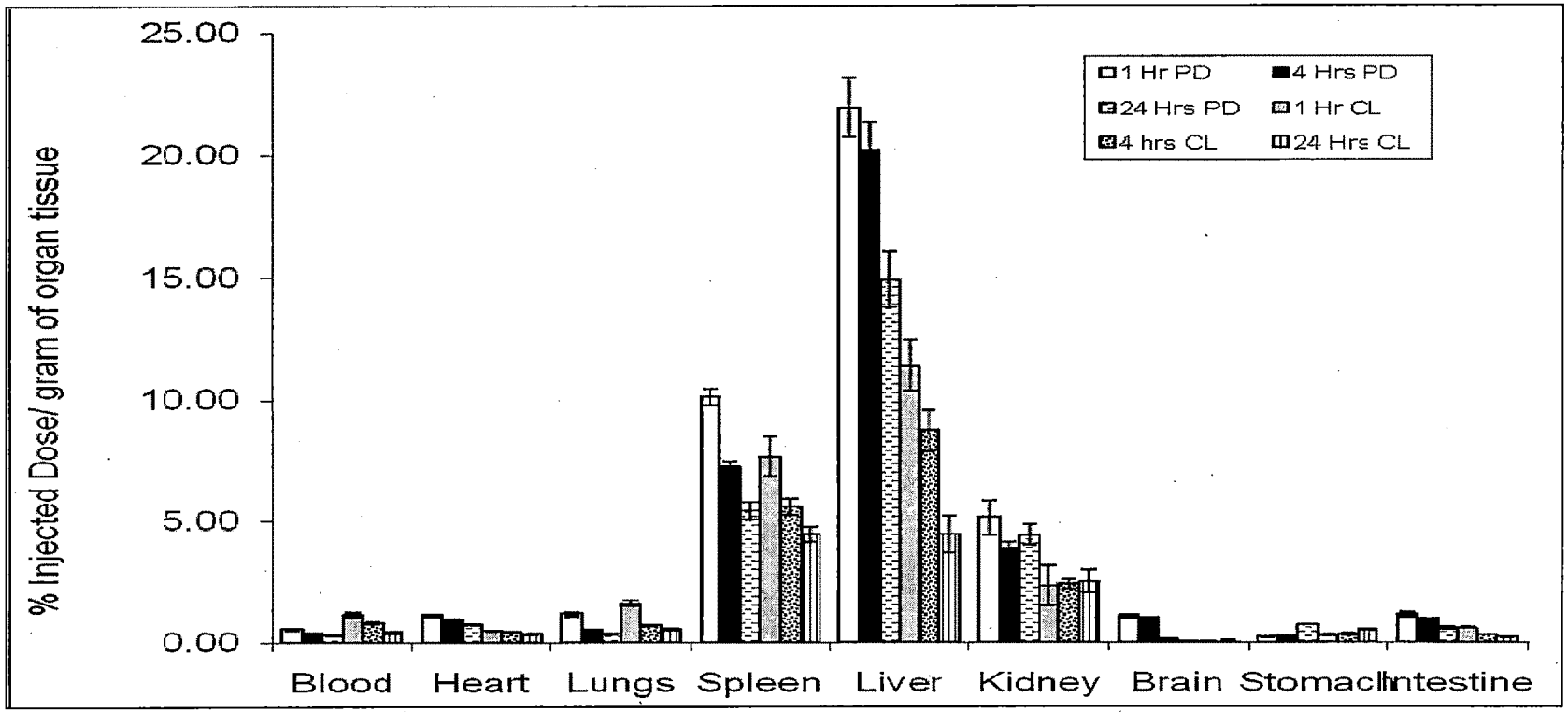

Figure 7.1 ^{99m}Tc labeled PD and CL was injected via tail vein in Swiss mice. Animals were sacrificed 1, 4 and 24 hrs post injection, all major organs and tumor was excised, rinsed in saline, wiped dry, weighed. Blood was withdrawn just before sacrificing the animal. Radioactivity associated with organs as well blood was measured in solid scintillation counter. Percentage of injected dose associated with per gram of tissue or organ was calculated. The values represented here are the mean of three values for each time point with ± standard deviation

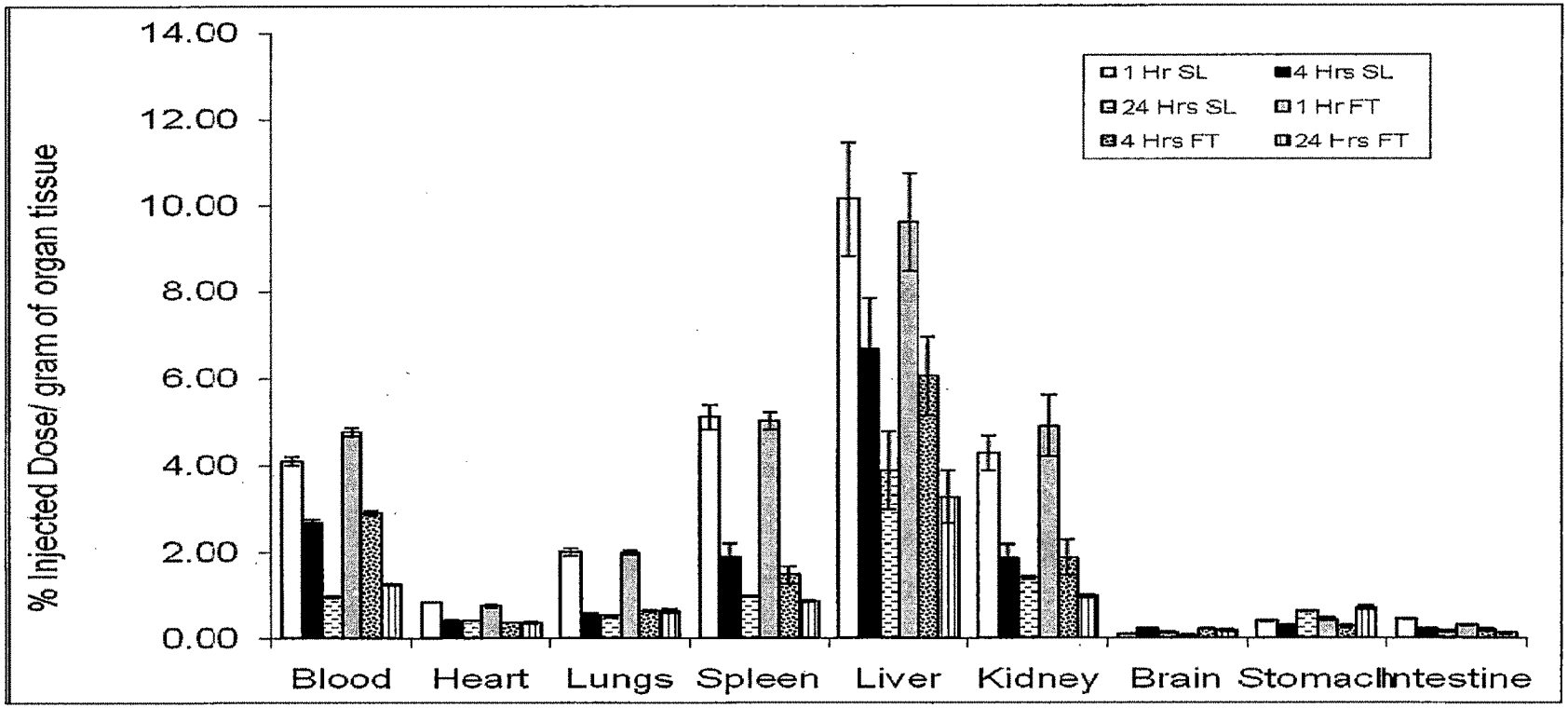

Figure 7.2 ^{99m}Tc labeled SL and FT was injected via tail vein in Swiss mice. Animals were sacrificed 1, 4 and 24 hrs post injection, all major organs and tumor was excised, rinsed in saline, wiped dry, weighed. Blood was withdrawn just before sacrificing the animal. Radioactivity associated with organs as well blood was measured in solid scintillation counter. Percentage of injected dose associated with per gram of tissue or organ was calculated. The values represented here are the mean of three values for each time point with ± standard deviation

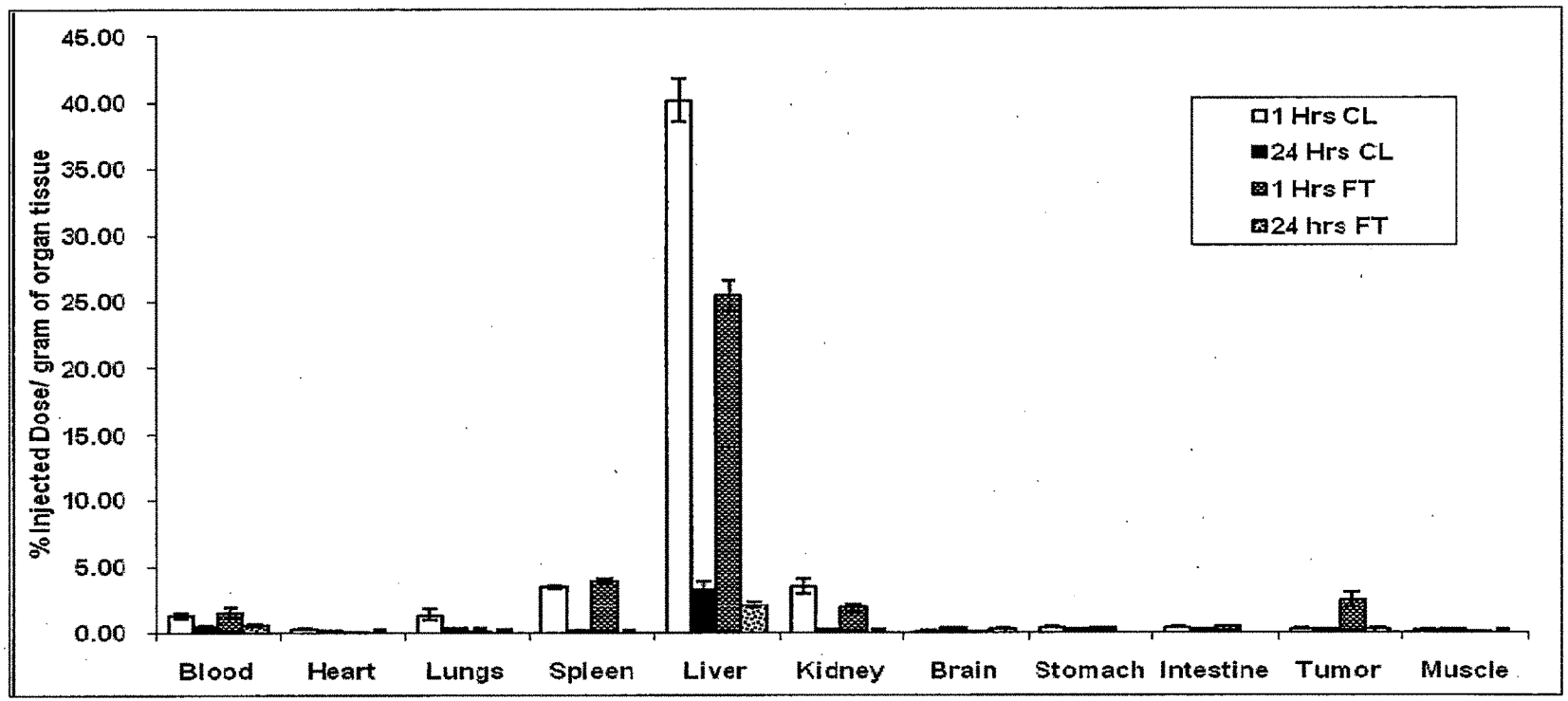

Figure 7.3: ^{99m}Tc labeled CL and FT was injected via tail vein in tumor bearing Swiss mice. Animals were sacrificed 1 and 24 hrs post injection, all major organs and tumor was excised, rinsed in saline, wiped dry, weighed. Blood was withdrawn just before sacrificing the animal. Radioactivity associated with organs as well blood was measured in solid scintillation counter. Percentage of injected dose associated with per gram of tissue or organ was calculated. The values represented here are the mean of three values for each time point with ± standard deviation

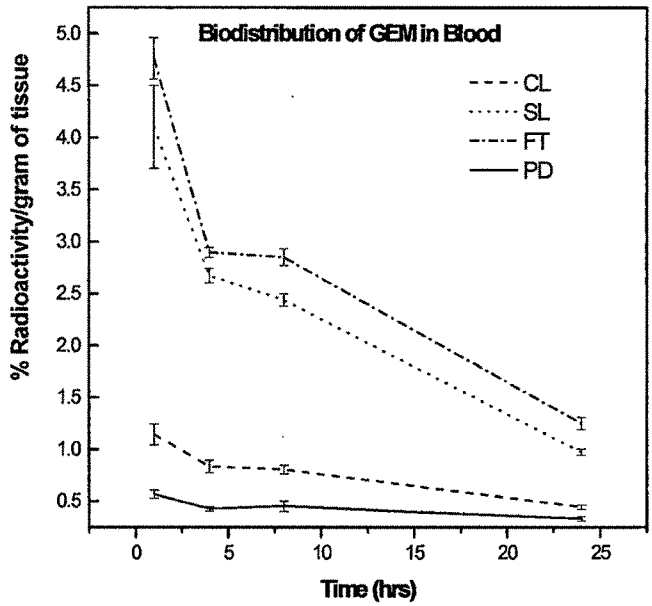

Figure 7.4 Blood concentration versus time plot following administration of ^{99m}Tc-GEM formulations

Table 7.7 Pharmacokinetics of ^{99m}Tc-CL/SL/FT/PD of blood in Swiss mice

Formulation	AUC 0→24 hrs (hours × % radioactivity/g)	β(terminal) (hours^{-1})	liver:blood ratio at 1 hr	liver:blood ratio at 4 hr	liver:blood ratio at 24 hr
CL	17.02	0.036848	9.93	10.41	10.03
SL	49.70	0.050666	2.47	2.50	3.99
FT	58.31	0.057575	2.01	2.08	2.61
PD	9.96	0.018424	38.61	47.25	45.43

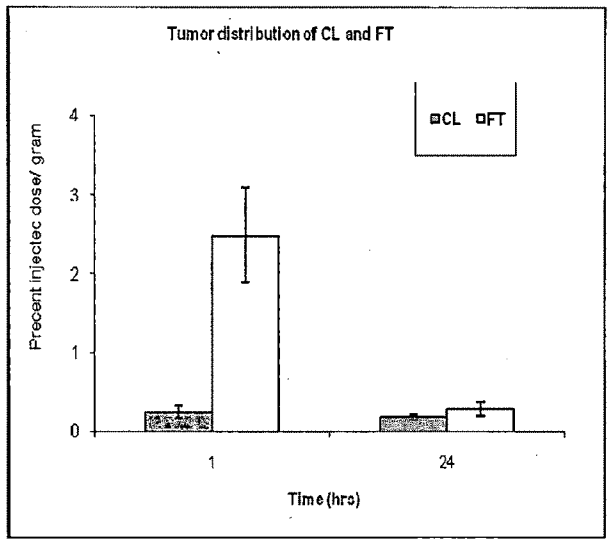

Figure 7.5 Tumor distribution of CL and FT in tumor bearing mice after intravenous injection. Tumor was isolated after 1 and 24 hrs of post injection and estimated for the radioactivity. Radioactivity is expressed as percent of administered dose per gram of tissue or organ. The values are mean of three mice with ±SD

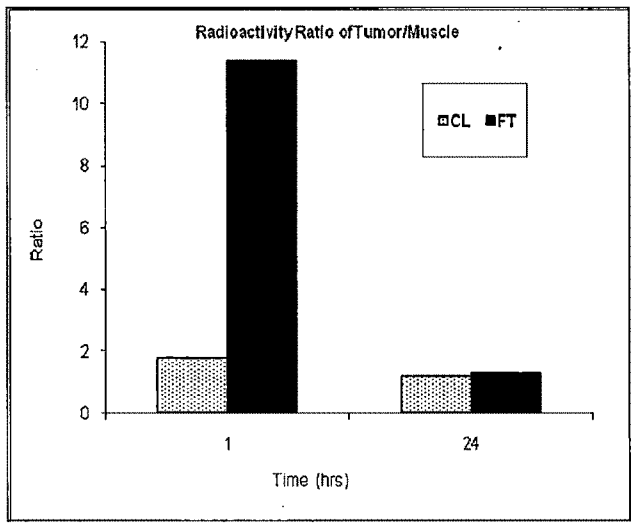

Figure 7.6 Ratio of tumor to muscle uptake of CL and FT in tumor induced mice after 1 and 24 hrs of post injection

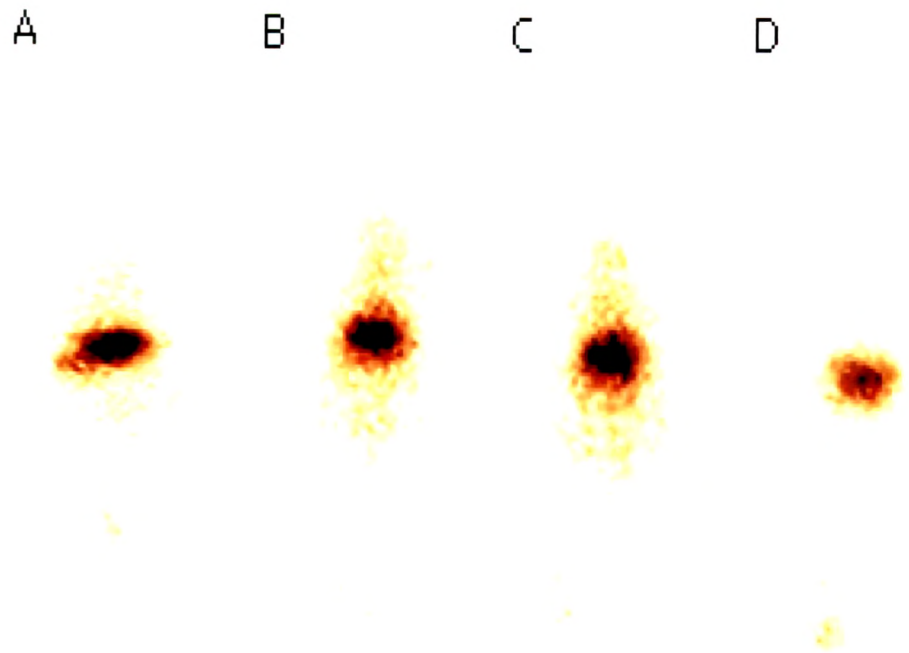

Figure 7.7 Gamma scintigraphic images of a mice with ^{99m}Tc-labeled liposomes 1 hr post treatment (A) Conventional liposomes (B) Stealth liposomes (C) Folate targeted liposmes (D) Pure drug

7.10 Results and Discussion

7.10.1 Biodistribution in Swiss mice

Gemcitabine formulations (CL, SL, FT, PD) were radiolabeled by direct labeling method. The radiolabeling was optimized by consideration of three factors such as amount of stannous chloride, incubation time/ *in vitro* stability of the radiolabeled complex and pH. The pH was adjusted ranging from 6 -7.5 and the amount of stannous chloride for optimum labeling (Theobald, 1990; Saha, 1993; Saha, 2005) was studied and the results were shown in Table 7.1. The stability studies of ^{99m}Tc-CL/SL/FT/PD were carried out *in vitro* using normal saline and mice serum by ascending ITLC (Garron et al., 1991), *in vitro* stability of the complexes for 24hours was assessed and the results were shown in Table 7.2. The bonding strength of ^{99m}Tc-CL/SL/FT/PD was assessed by DTPA (Diethylene triamine penta acetic acid) challenging test (Babbar et al., 2000; Saha, 2005). The effect of different molar concentrations of DTPA on ^{99m}Tc- CL/SL/FT/PD and percent transchelation were studied and given in Table 7.3. The GEM formulations were labeled successfully and

their radio chemical purity/ labeling efficiency were found to be more than 90%. The radiolabeled ^{99m}Tc- CL/SL/FT/PD complexes were found to be stable in normal saline and mice serum only with less than 10% degradation over 24 hours. The percent transchelation of ^{99m}Tc- CL/SL/FT/PD were found to be less than 4% with 4mM DTPA.

Biodistribution of ^{99m}Tc- CL/SL/FT/PD following i.v. administration in swiss mice were performed and the radioactivity was estimated at predetermined time intervals up to 24hours. The results obtained are recorded in Table 7.5-7.6. The biodistribution of GEM in blood following i.v of ^{99m}Tc- CL/SL/FT/PD were shown in Figure 7.1-7.2. The pharmacokinetic parameters like AUC and terminal elimination rate constant were calculated using standard pharmacokinetic principles and given in Table 7.7.

The enhancement of AUC in blood followed by i.v admistration of FT and SL are in congruence with the observations reported by Lianli et al., 2002 and Zhang et al., 2004, that liposomes enhances the transport of drug across tumor. Calculating the radioactivity in whole blood after 1, 4 and 24 hrs, we observed that both SL and FT followed nearly the same pattern of blood clearance (Figure 7.2) till 4 hrs. But FT was retained higher in blood compared to SL at 24 hrs, this may be because of higher liver uptake of SL compared to FT.

In case of ^{99m}Tc labeled PD, liver and spleen accumulated a major portion of the administered radioactivity as they are the two major organs of reticuloendothelial system (RES) which are known to accumulate and metabolize (Semple et al., 1998; Monica et al., 2000). The biodistribution data reveals higher initial rapid uptake by liver, which was 21.932±0.22 for PD after 1 hr of post injection (Liu and Liu., 1996; Liu, 1997). Radioactivity of liposomes in liver after 1, 4 and 24 hrs was very less compare to PD in liver as shown in table 7.5. The possible reason for higher retention of PD in liver and spleen would be because of higher cellular uptake this can be also observed in the gamma scintigraphic images of PD in mice after intravenous administration (Fig 7.6).

7.10.2 Biodistribution in Tumor

Uptake of radiolabeled CL and FT liposomes were compared in tumor (Ehrlich carcinoma) induced mice after 1 and 24 hrs of injection. The characterization of developed Ehrlich carcinoma for folate receptor expression was not carried out due to practical difficulties. Earlier studies have reported that folate targeted liposomes were highly taken up by the *in vivo* tumor cells expressing high amount of folate receptor (Gabizon et al., 2003). The relevance of folate receptor as a useful target for tumor-specific drug delivery is supported by findings indicating up-regulation (higher expression) in many human cancers including those of the ovary, brain, kidney, lung, breast and myeloid cells etc. In addition, aggressive or undifferentiated tumors with advanced stage or grade appear to have an increased folate receptor density suggesting that folate receptor mediated delivery may be a broad approach in targeting tumor cells (Toffoli et al., 1997). We have already observed the enhanced uptake of FT *in vitro* on HeLa cell lines compared to A549 used in uptake studies (Figure from *in vitro* uptake studies 6.5, 6.6).

Considering this we intended to study the uptake of FT by Ehrlich carcinoma tumor cells, this study would make us understand the effect of modified surface property of liposome on tumor uptake. The results of tumor uptake obtained in tumor induced mice for FT and CL are shown in table 7.6 and figure 7.3. The tumor uptake of FT was 2.49 and 0.28 % and for CL was 0.25 and 0.18 % after 1 and 24 hrs respectively. Tumor uptake of FT was higher compared to CL at 1 hrs and remained higher at 24 hrs as shown in figure 6.4.

To compare the targeting profile of FT with CL, we examined tumor-to-normal tissue (muscle) uptake ratio. Tumor: plasma uptake ratios are not presented as they are not pharmacodynamically relevant because the liposomes present in plasma are still in a distribution phase. The uptake ratio of tumor to muscle was 11.37 and 1.29 for FT and for CL 1.79 and 1.20 after 1 and 24 hrs post injection respectively. The tumor to muscle uptake ratio for FT increased after 1 hr then CL due to higher uptake and retention of FT in tumor (Figure 7.5). The higher uptake is because of surface modification of liposome by conjugation with folic acid, after 24 hrs was almost

similar, the possible reason to explain the measured FT and CL accumulation in tumor is the result based on the enhanced permeability and retention effect (Maeda, 2001).

7.10.3 Biodistribution by gamma imaging studies

Gamma scintigraphy imaging of mice administered with i.v. of ^{99m}Tc-CL/SL/FT/PD were performed. The gamma scintigraphy images of mice 1 hr post i.v. administration were shown in Figure 7.6. In case of PD accumulation of radioactivity in the mice RES was observed but in case of liposomal suspension distribution of radioactivity was observed following different formulations given by i.v., the scintigraphy images were consistent with the findings of the biodistribution studies.

7.11 Conclusion

The biodistribution of ^{99m}Tc labeled CL/SL/FT/PD showed that the higher distribution PD in liver and spleen. Blood retention of liposomal suspension was more due to decreased RES uptake, while PD shows low blood retention, was lower radioactivity at 1 hr, indicating rapid clearance from the blood due to liver and spleen uptake. From the scintigraphic images it has been confirmed that higher retention of PD in RES and, distribution of liposomal suspension. Among this liposomal suspension FT shows more blood retention and AUC thereby it shows an improvement in tumor uptake it has been confirmed by tumor biodistribution, it shows that more tumor uptake takes place by FT liposomal suspension after 4 and 24 hrs of distribution study (Xiang et al., 2008). Tumor to muscle uptake ratio for FT was nearly 5 fold higher compared to CL indicating enhanced targeting efficiency to tumor. These results indicate that the improvement of tumor targeting takes place by FT liposomal delivery system.

Reference

1. Babbar AK, Singh AK, Goel HC, Chauhan UPS, Sharma RK. Evaluation of ^{99m}Tc labeled Photosan-3, a heamatoporphyrin derivative, as a potential radiopharmaceutical for tumor scintigraphy. Nucl Med Biol 2000;27:419–426.
2. Capala J, Barth RF, Bailey MQ et al, Radiolabeling of epidermal growth factor with 99m Tc and invivo localization following intracerebral injection into normal and glioma bearing rats. Bioconjug Chem 1997;8:289-295.
3. Eckelman WC. Radiolabeling with technetium-99m to study high-capacity and low-capacity biochemical systems. Eur. J. Nucl. Med.1995;22:249-263.
4. Garron JY, Moinereau M, Pasqualini R, Saccavini JC. Direct 99mTc labeling of monoclonal antibodies: radiolabeling and in-vitro stability. Int J Rad Appl Intru 1991;18:695-703.
5. Ishida O, Maruyama K, Sasaki K, Iwatsuru M. Size-dependent extravasation and interstitial localization of polyethyleneglycol liposomes in solid tumor-bearing mice. Int. J. Pharm. 1999;190:49-56.
6. Kamps AAM, Scherphof GL. Biodistribution and Uptake of Liposomes *in vivo*. Methods in Enzymology 2004;387:257-26.
7. Laverman P, Boermana OC, Wim JG, et al., Liposomes for scintigraphic detection of infection and inflammation, Adv. Drug Deliv. Rev. 1999;37:225-235.
8. Lianli, Indranil Nandi and Kim KH. Development of an ethyl laurate-based microemulsion for rapid-onset intranasal delivery of diazepam. Int J Pharmaceutics 2002; 237(1-2):77-85.
9. Liu D. Biological factors involved in blood clearance of liposomes by liver. Adv. Drug Deliv. Rev. 1997;24:201-213.
10. Liu F, Liu D. Serum independent liposome uptake by mouse liver. Biochim. Biophys. Acta 1996;1278:5-11.
11. Maeda H. The enhanced permeability and retention (EPR) effect in tumor vasculature: the key role of tumor-selective macromolecular drug targeting. Adv. Enzyme Regul. 2001;41:189–207.
12. Maruyama K. *In vivo* targeting by liposomes. Biol. Pharm. Bull. 2000; 23: 791-799.

13. Monica CD, Valerie B, Elias F, et al., Improvement of *in vivo* stability of phosphodiester oligonucleotide using anionic liposomes in mice. Life Sciences 2000;67:1625-1637.
14. Richardson VJ, Jeyasingh K, Jewkes RF et al., Possible tumor localization of 99m Technetium labeled liposomes: effects of lipid composition, charge, and liposome size. J. Nucl. Med. 1978;19:1049-1054.
15. Saha GB. Fundamentals of Nuclear Pharmacy, 5th edition, New York: Springer-Verlag; 2005.
16. Saha GB. Methods of Radiolabeling. Saha GB. Physics and Radiobiology of Nuclear Medicine. Springer; New York: 1993;100-106.
17. Semple SC, Chonn A, Cullis PR. Interactions of liposomes and lipid-based carrier systems with blood proteins: Relation to clearance behavior *in vivo*. Adv. Drug Deliv. Rev. 1998;32:3-17.
18. Theobald AE. Theory and practice. In: Sampson C, Editor. Text book of radiopharmacy. New York, NY: Gorden and Breach.1990;127-128.
19. Wu MS, Robbins JC, Ponpipom MM, Shen TV. Modified *in vivo* behavior of liposomes containing synthetic glycolipids. Biochim. Biophys. Acta 1981;674:19-29.
20. Xiang G, Wu J, Lu J, Liu Z, Lee RJ. Synthesis and Evaluation of A Novel Ligand for Folate-mediated Targeting liposomes. Int J Pharm. 2008;356(1-2):29–36.
21. Zhang Q, Jiang X, Xiang W, Lu W, Su L, Shi Z. Preparation of nimodipine-loaded microemulsion for intranasal delivery and evaluation of the targeting efficiency to brain. Int J Pharm. 2004;275:85-96.
22. Zhao Y, Yue P, Tao T, Chen QH. Drug brain distribution following intranasal administration of Huperzine A insitu gel in rats. Acta Pharmacologicaa sinica 2007;28(2):273-278.